Journal of Aeronautics & Aerospace Engineering
Yeh and Yeh, J Aeronaut Aerospace Eng 2014, 3:1
DOI: 10.4172/2168-9792.1000128
Research Article Open Access

A Dimensionless Analysis of Young's Modulus and Stress Distribution for Orthotropic Materials

Hsien-Liang Yeh[1]* and Hsien-Yang Yeh[2]

[1]*Department of Civil and Ecological Engineering, I-Shou University, Kaohsiung City 84001, Taiwan*
[2]*Department of Mechanical Engineering, California State University, Long Beach, Long Beach, CA 90840-8305, USA*

Abstract

The effect of various offaxis angles and lamina material properties on the axial and transverse modulus of the orthotropic lamina under off-axis loading is studied. Also, the stress distribution of the orthotropic composite plate containing a circular cutout with normal pressure distributed uniformly along the opening edge is investigated. Through the generalized Hooke's law and plane stress condition, a dimensionless analysis is used to evaluate the influence of various elastic moduli E_1, E_2, G_{12} and ν_{12} on the axial and transverse modulus of the orthotropic lamina under various off-axis loadings. Moreover, based on the generalized Hooke's law, the generalized plane stress and the complex variable method, a dimensionless analysis is used to evaluate the influence of various elastic moduli E_1, E_2, G_{12} and ν_{12} on the stress distribution along the boundary of the circular cutout of the orthotropic plate with normal pressure distributed uniformly along the opening edge. The results obtained from this dimensionless analysis provide a set of general design guidelines for structural laminates with high precision requirements in the engineering applications.

Keywords: Lamina; Axial and transverse modulus; Orthotropic plate; Complex variable; Offaxis angle; Stress distribution; Composite materials

Introduction

Composite materials consist of various fibrous reinforcements coupled with a compatible matrix to achieve superior structural performance. The selection of composite materials for specific applications is generally determined by the physical and mechanical properties of the materials, evaluated for both function and fabrication [1]. The axial and transverse modulus of a composite laminate is an important physical parameter in the application and testing of composite materials. Knowledge of stress distributions in anisotropic materials is very important for proper use of these new high-performance materials in structural applications [2].

Schulgasser and Page [3] considered the importance of the transverse or non-axial fiber properties in determining the in-plane elastic behavior of a paper sheet. Scott [4] defined a new modulus of elasticity to be the ratio of an equibiaxial stress to the relative area change of the planes in which the stress acts. This area modulus of elasticity is intermediate in properties between Young's modulus and the bulk modulus. Spencer [5] described a simple method which used axial and torsional vibration resonance for the measurement of Young's modulus, E, and shear modulus, G, of shafts. Zheng and Zhu [6] investigated the effect of an applied electric field on Young's modulus of nanowires. Upadhyay and Lyons [7] calculated effective elastic constants of three-phase composite with degraded interphase coating for the graphite/epoxy composite system.

Kuwamura [8] analyzed the stresses around the circular hole by means of Ikeda's formula in consideration of orthotropic elasticity of the woods, which revealed that the stresses distribution around the circular hole is nearly equal to that of an isotropic plate. Selivanov [9] studied the time variation in the stresses around an elliptic hole in a composite plate. Kumar and Rao [10] presented an approximate solution in the form of a polynomial for the normal stress distribution adjacent to a class of optimum holes in symmetrically laminated infinite composite plates under uniaxial loading. Giare and Shabahang [11] used a finite element analysis to calculate the stress distribution around a hole in a finite isotropic plate reinforced by composite materials. Tsai et al. [12] developed a novel procedure for predicting the notched strengths of composite plates each with a circular hole and the stress distribution of the circular cutout is obtained by a finite element analysis.

Methods and Materials

A dimensionless analysis model for evaluation of axial and transverse modulus

Based on the generalized Hooke's law and the related plane stress equations in the global coordinates, axial and transverse modulus, E_x and E_y, has been derived [13-18]. The transformed plane stress constitutive equations can be inverted to give [14-18].

$$\begin{Bmatrix} \varepsilon_x \\ \varepsilon_y \\ \gamma_{xy} \end{Bmatrix} = \begin{bmatrix} \bar{S}_{11} & \bar{S}_{12} & \bar{S}_{16} \\ \bar{S}_{12} & \bar{S}_{22} & \bar{S}_{26} \\ \bar{S}_{16} & \bar{S}_{26} & \bar{S}_{66} \end{bmatrix} \begin{Bmatrix} \sigma_x \\ \sigma_y \\ \tau_{xy} \end{Bmatrix} \tag{1}$$

The unidirectional off-axis lamina under the loading $\sigma_x \neq 0$ with $\sigma_y = \tau_{xy} = 0$, as depicted in Figure 1, the axial modulus, E_x, can be written as [14-18].

$$E_x = \frac{1}{\bar{S}_{11}} = \frac{E_1}{\left[\cos^4\alpha + \cos^2\alpha \sin^2\alpha \left(-2\nu_{12} + \frac{E_1}{G_{12}} \right) + \sin^4\alpha \frac{E_1}{E_2} \right]} \tag{2}$$

***Corresponding author:** Hsien-Liang Yeh, Department of Civil and Ecological Engineering, I-Shou University, Kaohsiung City 84001, Taiwan, Tel: 886-7-6577711; E-mail: hlyeh@isu.edu.tw

Received February 06, 2014; **Accepted** March 24, 2014; **Published** April 01, 2014

Citation: Yeh HL, Yeh HY (2014) A Dimensionless Analysis of Young's Modulus and Stress Distribution for Orthotropic Materials. J Aeronaut Aerospace Eng 3: 128. doi:10.4172/2168-9792.1000128

Citation: Yeh HL, Yeh HY (2014) A Dimensionless Analysis of Young's Modulus and Stress Distribution for Orthotropic Materials. J Aeronaut Aerospace Eng 3: 128. doi:10.4172/2168-9792.1000128

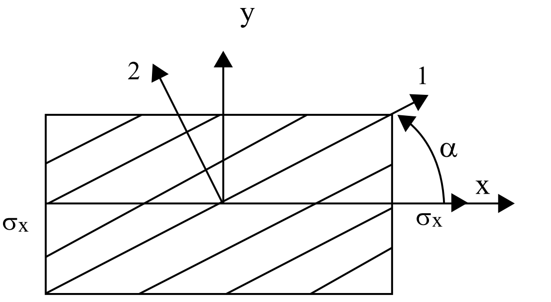

Figure 1: Off-Axis Lamina under Tensile Stress.

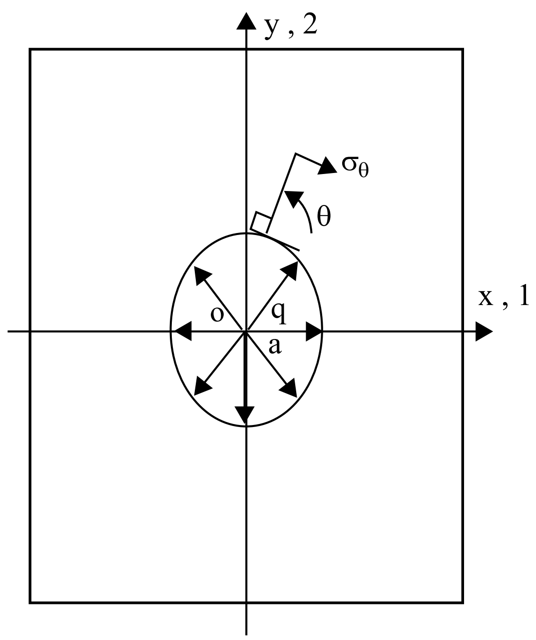

Figure 2: An orthotropic plate containing a circular hole under normal pressure distributed uniformly along the opening edge with principal material axes 1-2 and x-y axes.

Similarly, the transverse modulus, E_y, can be written as [14-18]

$$E_y = \frac{E_1}{\left[\sin^4\alpha + \cos^2\alpha \sin^2\alpha \left(-2\nu_{12} + \frac{E_1}{G_{12}}\right) + \cos^4\alpha \frac{E_1}{E_2}\right]} \qquad (3)$$

Consider the unidirectional off-axis lamina under the loading $\sigma_x \neq 0$ and the off-axis angle α varying from -90° to 90°. For a dimensionless analysis, three lamina material constants E_1, E_2 and G_{12} are represented by two dimensionless ratios E_2/E_1 and G_{12}/E_1. Totally, the lamina material has three parameters E_2/E_1, G_{12}/E_1 and ν_{12}. For an unidirectional off-axis lamina with different values of E_2/E_1, G_{12}/E_1, ν_{12} and α, the axial and transverse modulus of the lamina under the off-axis loading will vary and provide different values.

Various cases of different combinations of three material parameters are considered in this study. In general case, the ranges of E_2/E_1 and G_{12}/E_1 are between zero and one, the ranges of ν_{12} are between 0 and 0.6. For a lamina with given material properties E_2/E_1, G_{12}/E_1 and ν_{12} as well as the off-axis angle α, the axial and transverse modulus in the lamina under off-axis loading can be evaluated.

Tangential stresses on the boundary of the circular opening

The stress-strain distribution of an infinite anisotropic plate containing a through-the-thickness cutout has been derived using a complex variable method [19-21]. For an orthotropic plate subjected to normal pressure q distributed uniformly along the opening edge as shown in Figure 2. The normal stress component σ_θ for an element tangential to the opening is [20]

$$\sigma_\theta = q\frac{E_\theta}{E_1}[-k+n(\sin^2\theta + k\cos^2\theta) + (1+\mu_1^2)(1+\mu_2^2)\sin^2\theta\cos^2\theta] \qquad (4)$$

where

$$k = \sqrt{\frac{E_1}{E_2}} \qquad (5)$$

$$n = \sqrt{\frac{E_1}{G_{12}} - 2\nu_{12} + 2\sqrt{\frac{E_1}{E_2}}} \qquad (6)$$

$$\mu_1\,\mu_2 = -\sqrt{\frac{E_1}{E_2}} \qquad (7)$$

$$\mu_1^2 + \mu_2^2 = 2\nu_{12} - \frac{E_1}{G_{12}} \qquad (8)$$

The θ is the polar angle measured from the x-axis; E_θ is the Young's modulus tension (compression) in the direction tangent to the opening contour, which is related to elastic constants in the principal directions by the formula [20].

$$\frac{1}{E_\theta} = \frac{\sin^4\theta}{E_1} + \left(\frac{1}{G_{12}} - \frac{2\nu_{12}}{E_1}\right)\sin^2\theta\cos^2\theta + \frac{\cos^4\theta}{E_2} \qquad (9)$$

For an isotropic plate [20]

$$\sigma_\theta = q \qquad (10)$$

A dimensionless analysis model for evaluation of the normal stress σ_θ

Consider the orthotropic plate with a circular hole subjected to normal pressure q distributed uniformly along the opening edge. For a dimensionless analysis, three lamina material constants E_1, E_2 and G_{12} are represented by two dimensionless ratios E_2/E_1 and G_{12}/E_1. Totally, the lamina material has three parameters E_2/E_1, G_{12}/E_1 and ν_{12}. For a unidirectional lamina with different values of E_2/E_1, G_{12}/E_1 and ν_{12}, the normal stress component σ_θ of the orthotropic plate under normal pressure q distributed uniformly along the opening edge will vary and provide different values.

Various cases of different combinations of three material parameters are considered in this study. In general case, the ranges of E_2/E_1 and G_{12}/E_1 are between zero and one, the ranges of ν_{12} are between 0 and 0.6. For a lamina with given material properties E_2/E_1, G_{12}/E_1 and ν_{12}, the normal stress component σ_θ of the orthotropic plate under normal pressure q distributed uniformly along the opening edge can be evaluated.

Results and Discussion

Since the variation of the axial modulus E_x is bilateral symmetry to the off-axis angle α=0, the variation of the axial modulus E_x is considered

Citation: Yeh HL, Yeh HY (2014) A Dimensionless Analysis of Young's Modulus and Stress Distribution for Orthotropic Materials. J Aeronaut Aerospace Eng 3: 128. doi:10.4172/2168-9792.1000128

only in the range of 0° ≤ α ≤ 90°. Also, the curves of transverse modulus E_y are identical to those for E_x, but shifted 90°. Thus, only the variation of the axial modulus E_x is considered.

Given E_1=204GPa, G_{12}/E_1=0.2 and ν_{12}=0.2, the variations of the axial modulus E_x with off-axis angle α and different values of E_2/E_1 are shown in Figure 3. For different off-axis angle α and various values of E_2/E_1 from 0.2 to 0.4, the axial modulus E_x varies first from the maximum value at α=0° then decreases to the minimum values at α=90° as shown in Figure 3. But for E_2/E_1=0.6, with different off-axis angle α, the axial modulus Ex varies first from the maximum value at α=0° then decreases to the minimum value at α=60° and then increases to a large value at α=90°as shown in Figure 3. As for E_2/E_1=0.8 with different off-axis angle α, the axial modulus E_x varies first from the maximum value at α=0° then decreases to the minimum value at α=45° and then increases to a large value at α=90° as shown in Figure 3. Finally, for E_2/E_1=1.0,

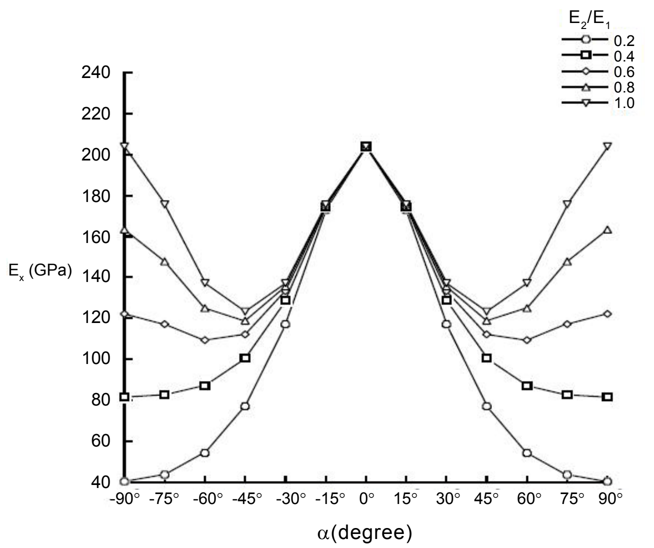

Figure 3: Lamina axial modulus Exvs. α and E_2/E_1 for E_1=204GPa, G_{12}/E_1=0.2, ν_{12}= 0.2.

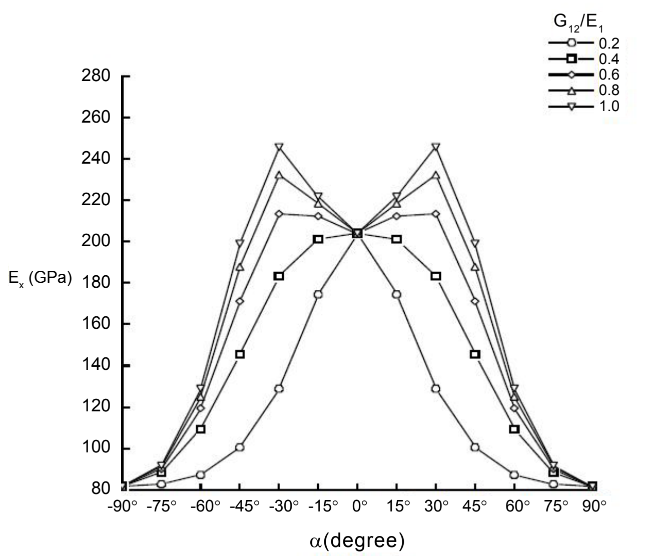

Figure 4: Lamina axial modulus Ex vs. α and G_{12}/E_1 for E_1=204GPa, E_2/E_1=0.4, ν_{12}=0.2.

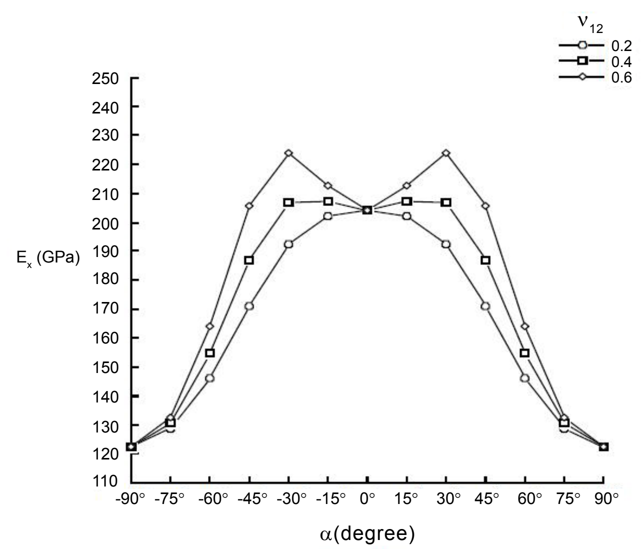

Figure 5: Lamina axial modulus Ex vs. α and ν_{12} for E_1=204GPa, E_2/E_1=0.6, G_{12}/E_1=0.4.

with different off-axis angle α, the axial modulus E_x varies first from the maximum value at α=0° then decreases to the minimum value at α=45° and then increases to the maximum value at α=90° as shown in Figure 3.

Given E_1=204GPa, E_2/E_1=0.4 and ν_{12}=0.2, the variations of axial modulus E_x with off-axis angle α and different values of G_{12}/E_1 are shown in Figure 4. For different off-axis angle α and various values of G_{12}/E_1 from 0.2 to 0.4, the axial modulus E_x varies first from the maximum value at α=0° then decreases to the minimum values at α=90° as shown in Figure 4. As for the changed values of G_{12}/E_1 from 0.6 to 1.0, with different off-axis angle α, the axial modulus E_x varies first from a large value at α=0° then increases to the maximum value at α=30° and then decreases to the minimum value at α=90° as shown in Figure 4.

Given E_1=204GPa, E_2/E_1=0.6 and G_{12}/E_1=0.4, the variations of the axial modulus E_x with off-axis angle α and different values of ν_{12} are shown in Figure 5. With different off-axis angle α and ν_{12}=0.2, the axial modulus E_x varies first from the maximum value at α=0° then decreases to the minimum value at α=90° as shown in Figure 5. As for the changed values of ν_{12} from 0.4 to 0.6, with different off-axis angle α, the axial modulus E_x varies first from a large value at α=0° then increases to the maximum value at α=30° and then decreases to the minimum value at α=90° as shown in Figure 5.

In the Figures 6-8, the bold solid line represents the circular hole and the bold dotted line shows the stress distribution σ_θ in an isotropic plate subjected to identical load as in an orthotropic plate. Since the stress distribution for an orthotropic plate is symmetrical with respect to the opening center, the variation of the stress distribution σ_θ is considered only in the range of 0° ≤ θ ≤ 180° for an orthotropic plate. In an isotropic plate given q=100 MPa, then calculated from Equation (10), the constant stress σ_θ is 100 Mpa.

In Figure 6 given q=100 MPa, E_1=204 GPa, E_2/E_1=0.6 and G_{12}/E_1=0.4, the variation of the stress σ_θ with respect to the polar angle θ and ν_{12} is the following:

With ν_{12}=0.2, 0.4, and 0.6, the minimum corresponding stresses σ_θ are 87.28 Mpa, 77.83 Mpa, and 67.93 Mpa at θ=90° respectively, and the

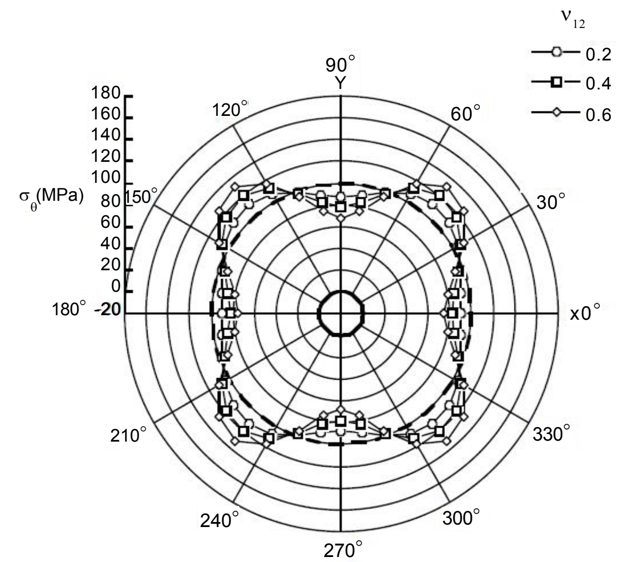

Figure 6: The normal stress component σ_θ vs. θ and ν_{12} for q=100MPa, E_1=204GPa, E_2/E_1=0.6 and G_{12}/E_1=0.4.

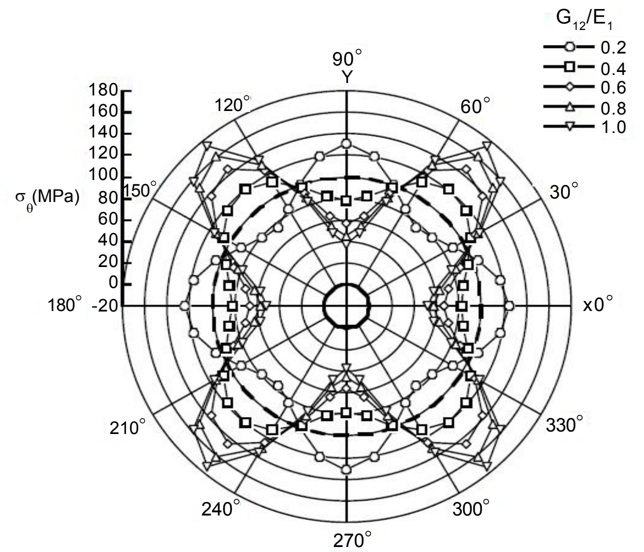

Figure 7: The normal stress component σ_θ vs. θ and G_{12}/E_1 for q=100MPa, E_1=204GPa, E_2/E_1=0.6 and ν_{12}=0.4.

maximum stresses σ_θ are 111.62 Mpa, 121.17 Mpa, and 132.14 Mpa at θ=50° and θ=130° respectively. Also, the stress concentration factors are S_c=1.12, 1.21, and 1.32 respectively, for orthotropic case. Figure 6 shows that within the ranges of the polar angle 0° ≤ θ ≤ 20°, 70° ≤ θ ≤ 110° and 160° ≤ θ ≤ 180°, the stress σ_θ decreases along with the increased values of ν_{12} respectively. But, in the ranges of the polar angle 30° ≤ θ ≤ 60° and 120° ≤ θ ≤ 150°, the stress σ_θ increases along with the increased values of ν_{12}.

In Figure 7 given q=100 MPa, E_1=204 GPa, E_2/E_1=0.6 and ν_{12}=0.4, the variation of the stress σ_θ with respect to the polar angle θ and G_{12}/E_1 is following:

For G_{12}/E_1=0.2, the minimum corresponding stresses σ_θ are 76.16 Mpa at θ=50° as well as θ=130°, and for G_{12}/E_1=0.4, 0.6, 0.8 and 1.0, the minimum corresponding stresses σ_θ are 77.83 Mpa, 56.61 Mpa, 45.03 Mpa and 37.69 Mpa at θ=90° respectively. With G_{12}/E_1=0.2, the maximum stresses σ_θ are 124.26 Mpa at θ=0° as well as θ=180°, and with G_{12}/E_1=0.4, 0.6, 0.8 and 1.0, the maximum stresses σ_θ are 121.17 Mpa, 146.09 Mpa, 162.21 Mpa and 173.54 Mpa at θ=50° as well as θ=130° respectively. Also, the stress concentration factors are S_c=1.24, 1.21, 1.46, 1.62, and 1.73 respectively, for orthotropic case. Figure 7 indicates that within the ranges of the polar angle 0° ≤ θ ≤ 20°, 70° ≤ θ ≤ 110° and 160° ≤ θ ≤ 180°, the stress σ_θ decreases along with the increased values of G_{12}/E_1 respectively. But, within the ranges of the polar angle 30° ≤ θ ≤ 60° and 120° ≤ θ ≤ 150°, the stress σ_θ increases along with the increased values of G_{12}/E_1.

In Figure 8 given q=100 MPa, E_1=204 GPa, G_{12}/E_1=0.6 and ν_{12}= 0.4, the variation of the stress σ_θ with respect to the polar angle θ and E_2/E_1 is following:

With E_2/E_1=0.2, 0.4, 0.6, 0.8 and 1.0, the minimum corresponding stresses σ_θ are 7.45 Mpa, 42.61 Mpa, 56.61 Mpa, 64.34 Mpa and 69.31 Mpa at θ=90° respectively, and the maximum stresses σ_θ are 177.49 Mpa, 157.60 Mpa, 146.09 Mpa, 138.66 Mpa and 133.47 Mpa at θ=50° and θ=130° respectively. Moreover, for E_2/E_1=1.0, the minimum stresses σ_θ occurred at θ=0° and θ=180° and the maximum stresses σ_θ occurred at θ=40° and θ=140° as well. Also, the stress concentration factors are S_c=1.77, 1.58, 1.46, 1.39, and 1.33 respectively, for orthotropic case. Figure 8 shows that within the ranges of the polar angle 0° ≤ θ ≤ 30°, 80° ≤ θ ≤ 100° and 150° ≤ θ ≤ 180°, the stress σ_θ increases along with the increased values of E_2/E_1 respectively. But, in the ranges of the polar angle 40° ≤ θ ≤ 60° and 120° ≤ θ ≤ 140°, the stress σ_θ decreases along with the increased values of E_2/E_1. As for the polar angles both θ=70° and θ=110°, with the various values of E_2/E_1 from 0.2 to 0.6 the stress σ_θ decreases along with the increased values of E_2/E_1, but with the various values of E_2/E_1 from 0.6 to 1.0 the stress σ_θ increases along with the increased values of E_2/E_1.

Conclusions

The effect of various offaxis angles and lamina material properties on the axial and transverse modulus of the orthotropic lamina

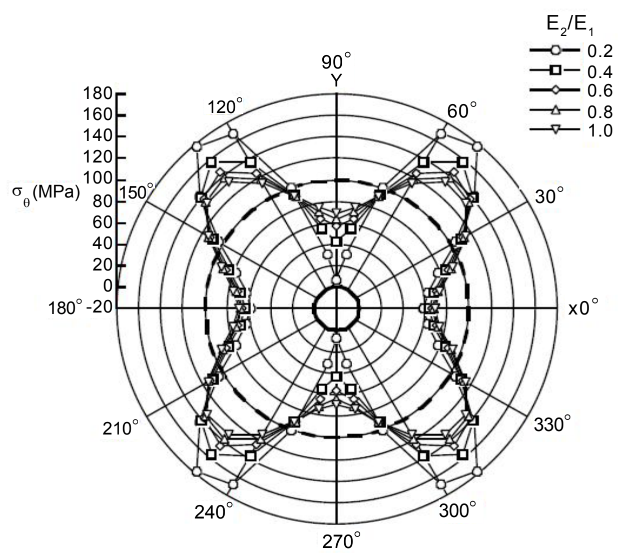

Figure 8: The normal stress component σ_θ vs. θ and E_2/E_1 for q=100MPa, E_1=204GPa, G_{12}/E_1=0.6 and ν_{12}=0.4.

under off-axis loading is studied. Also, the stress distribution of the orthotropic composite plate containing a circular cutout under normal pressure distributed uniformly along the opening edge is investigated.

First remark, given the fixed off-axis angle α and other fixed material parameters Figure 3 shows that the values of the lamina axial modulus Ex increase along with the increase values of E_2/E_1 except at α=0°.

Second remark, given the fixed off-axis angle α and other fixed material parameters Figure 4 shows that the values of the lamina axial modulus E_x increase along with the increase of the values of G_{12}/E_1 except for α=0° and α=90°.

Third remark, given the fixed off-axis angle α and other fixed material parameters, Figure 5 indicates that the values of the lamina axial modulus E_x increase along with the increase of the values of ν_{12} except at α=0°and α=90°.

Fourth remark, given other fixed material parameters Figures 6 and 8 indicates that within the ranges of the polar angle $0° \leq \theta \leq 90°$, the stress σ_θ varies first from a small value at θ=0° then increases to the maximum value at θ=50° and then decreases to the minimum value at θ=90°. But within the ranges of the polar angle $90° \leq \theta \leq 180°$, the stress σ_θ varies first from the minimum value at θ=90° then increases to the maximum value at θ=130° and then decreases to a small value at θ=180° as shown in Figures 6 and 8.

Fifth remark, given other fixed material parameters Figure 7 indicates that for the value of G_{12}/E_1=0.2, within the range of the polar angles $0° \leq \theta \leq 90°$, the stress σ_θ varies first from a large value at θ=0° then decreases to the minimum value at θ=50° and then increases to the maximum value at θ=90°. But within the ranges of the polar angle $90° \leq \theta \leq 180°$, the stress σ_θ varies first from the maximum value at θ=90° then decreases to the minimum value at θ=130° and then increases to a large value at θ=180° as shown in Figure 7. As for the values of $0.4 \leq G_{12}/E_1 \leq 1.0$, within the range of the polar angles $0° \leq \theta \leq 90°$, the stress σθ varies first from a small value at θ=0° then increases to the maximum value at θ=50° and then decreases to the minimum value at θ=90°. But within the ranges of the polar angle $90° \leq \theta \leq 180°$, the stress σ_θ varies first from the minimum value at θ=90° then increases to the maximum value at θ=130° and then decreases to a small value at θ=180° as shown in Figure 7.

The results obtained from this dimensionless analysis provide a set of general design guidelines for structural laminates with high precision requirements in the engineering applications.

References

1. Niu MCY (1992) Composite Airframe Structures. Hong Kong Conmilit Press limited USA.
2. Sadd MH (2009) Elasticity: Theory, Applications, and Numerics. Academic Press USA.
3. Schulgasser K, Page DH (1988) The influence of tranversefibre properties on the in-plane elastic behaviour of paper. Compos SciTechnol 32: 279-292.
4. Scott NH (2000) An Area Modulus of Elasticity: Definition and Properties. J Elasticity 58: 269-275.
5. Spencer A (1987) Young's modulus and shear modulus of a composite shaft from resonance measurements. Compos SciTechnol 28: 173-191.
6. Zheng X, Zhu L (2006) Theoretical analysis of electric field effect on Young's modulus of nanowires. ApplPhysLett 89.
7. Upadhyay PC, Lyons JS (2009) Elastic Constants of Uniaxially Fiber-Reinforced Composites with Degraded Interphase. J ReinfPlast Comp 28: 1441-1458.
8. Kuwamura H (2010) Splitting of Wood by Pressure in a Circular Hole: Study on Steel-Framed Timber Structures part 5. J StructEng 75: 175-184.
9. Selivanov MF (2010) Influence of the viscoelastic properties of a composite on the stress distribution around an elliptic hole in a plate. IntApplMech 46: 799-805.
10. Kumar RR, Rao GV (1994) Normal stress distribution adjacent to optimum holes in composite plates. Compos Struct 29: 393-398.
11. Giare GS, Shabahang R (1989) The reduction of stress concentration around the hole in an isotropic plate using composite materials. EngFractMech 32: 757-766.
12. Tsai KH, Hwan CL, Lin MJ, Huang YS (2012) Finite Element Based Point Stress Criterion for Predicting the Notched Strengths of Composite Plates. Journal of Mechanics 28: 401-406.
13. Love AEH (1892) A Treatise on the Mathematical Theory of Elasticity. Cambridge University Press, London.
14. Herakovich CT (1998) Mechanics of Fibrous Composites. John Wiley & Sons Inc USA.
15. Agarwal BD, Broutman LJ, Chandrashekhara K (2006) Analysis and Performance of Fiber Composites. John Wiley & Sons USA.
16. Jones RM (1998) Mechanics of Composite Materials. CRC Press UK.
17. Gibson RF (2011) Principles of Composite Material Mechanics. CRC Press USA.
18. White SR (1998) Stress Analysis of Fiber-Reinforced Composite Materials. McGraw-Hill Higher Education USA.
19. Sih GC, Paris PC, Irwin GR (1965) On cracks in rectilinearly anisotropic bodies. Int J Fracture 1: 189-203.
20. Lekhnitskii SG (1968) Anisotropic Plates. Gordon and Breach USA.
21. Tan SC (1994) Stress Concentrations in Laminated Composites. CRC Press USA.